

# DEVELOPMENT OF A MOBILITY DRIVE UNIT FOR LOW GRAVITY PLANETARY BODY EXPLORATION

J. Reill, H.-J. Sedlmayr, S. Kuß, P. Neugebauer, M. Maier, A. Gibbesch, B. Schäfer, and A. Albu-Schäffer

*DLR (German Aerospace Center), Robotics and Mechatronics Center, Muenchner Str. 20, 82234 Wessling, Germany  
E-mail: Josef.Reill@dlr.de*

## ABSTRACT

The 10 kg asteroid lander package MASCOT (mobile asteroid surface scout), developed by DLR, is a contribution to the JAXA Hayabusa-II mission, intended to be launched in 2014. MASCOT will provide in-situ surface science at several sites on the C-type asteroid 1999 JU3. An innovative hopping mechanism, developed at the Robotics and Mechatronics Center (RMC) in Oberpfaffenhofen, allows the lander to upright to nominal position for measurements as well as to relocate by hopping. The mechanism concept considers the uncertain and harsh environment conditions on the asteroid surface by using the impulse of an eccentric mass with all rotating parts completely inside the MASCOT structure. The paper gives an overview of the major development activities which lead to a new promising powerful and scalable drive system for low gravity planetary body exploration.

## 1. INTRODUCTION

The Robotics and Mechatronics Center (RMC) of DLR in Oberpfaffenhofen gained a lot of experience in terrestrial robotic systems as well as in in space applications. During the ROKVISS (robotics component verification on ISS) mission (see [1], [2] and [3]) there was a robotic arm built and launched towards the ISS in 2004. The robotic arm was telemanipulated with closed force feedback loop from ground while the robotic arm was mounted outside the ISS at the Zvezda service module. In 2011 the robotic arm was still working and returned to earth for further investigations. Several other powerful mechatronic systems with modular actuation units like the DEXHAND were built (see [4], [5] and [6]).

This paper shows a new developed hardware for the MASCOT landing unit, that was optimized to cope with the challenging requirements of the long term space mission Hayabusa-II. Especially the long cruise phase of approximately four years and additional eight months for target characterization is a big challenge for the hardware. During this time almost no movement of the mechatronic system is expected which contributes to the risk of cold welding within bearings and gear unit. Also thermal and

radiation issues have to be taken into account. The landing unit is about 10 kg and rectangular shaped with the size of 300 mm x 300 mm x 200 mm. There are several subunits of MASCOT:

- MASCOT structure (German Aerospace Center DLR Braunschweig FA-MFW, Germany)
- GNC, guidance, navigation & control system (German Aerospace Center DLR Bremen RY, Germany)
- PCDU, power and communication systems (CNES Centre National D'études Spatiales)
- OBC, on board computer (Telespazio VEGA Deutschland GmbH, Germany)
- CAM, visible camera (German Aerospace Center DLR Berlin PF, Germany)
- MARA, infrared radiometer (German Aerospace Center DLR Berlin PF, Germany)
- MAG, magnetometer (Technische Universität Braunschweig, Germany)
- MicroOmega, near infrared hyperspectral microscope (IAS Paris, France)
- MOB, mobility unit (German Aerospace Center DLR Oberpfaffenhofen RMC, Germany)

The integration of all subsystems and payloads is done at the DLR Institute of Space Systems, Exploration Systems in Bremen. In this paper the mobility mechanism hardware and electronics will be shown in detail. The other components and systems are presented in different other papers (see for example: [7]). Mission and decision details to the mechanism are presented in [8].

Functional safety aspects during the mission forced the realization of a redundant electronic block. Furthermore the 120 g mass of the eccentric arm must be accelerated and decelerated in a fast way which needs a strong drive. Both requirements are contrary to the given space and mass restrictions. The realized electronics including control, sensors and motor drive subsystems are realized on a single PCB, sized 95 mm x 105 mm in total for both redundancy paths. The system is designed for -55 up to 100°C storage and -40 up to 80°C operating temperature.

## 2. MOBILITY SYSTEM OVERVIEW

The mobility mechanism is based on the reactive force generated by an eccentric arm. This way MASCOT is able to hop on the asteroid surface. Solutions with drive wheels were rejected because of surface uncertainties and weight limitations.

In Fig. 1 the Simpack model structure of the Mascot mobility system is shown as implemented in the MBS formalism. By introducing the polygonal contact model approach (PCM) arbitrary surfaces can be modelled on the mobility and on the asteroid surface side. With the elastic layer contact and the multi-body system approach highly reliable simulation results are possible for hopping and uprighting manoeuvres. The asteroid gravitational force is implemented by means of the gravitational force law of Eq. 1

$$F = G \cdot \frac{m_{asteroid} \cdot m_{mascot}}{r^2} \quad (1)$$

with  $G = 6.6738410^{-11}$ , gravitational constant.

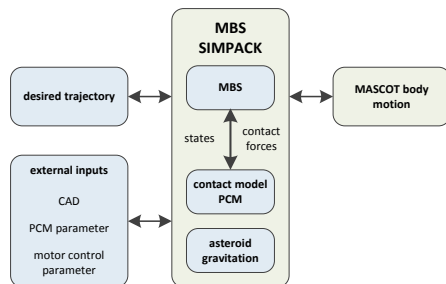


Figure 1. Mascot Simpack Architecture

A general overview of the mechanical system is given in Fig. 2. The MobCon on the left hand side represents the mobility controller that is described in more detail in Fig. 3. The drive unit consists of a brushless dc motor with very high power density and a high reliability because of only very few mechanical parts and the absence of brushes. The motor design was done by DLR while the manufacturing of the lightweight torque servo motor is actually done by RoboDrive [9] which is a DLR spin-off company. The motor is mounted to a harmonic drive gearing with a 1:30 reduction. For commutation reasons and also to calculate the position of the eccentric arm, digital hall sensors are used.

The electronics consists of two fully separated cold redundant signal paths. This concept enables the OBC to switch to the other redundancy path in case of some failure. Due to weight and volume restrictions the motor could not be realized redundant. Also the hall sensors in the motor housing are not redundant due to the very small motor outer diameter of 25 mm. To ensure functionality, radiation hard hall sensors are used. With the motor and the sensors being not redundant, the redundant electronics needs to be connected to the non redundant

motor and hall sensors by a special decoupling network (patent pending).

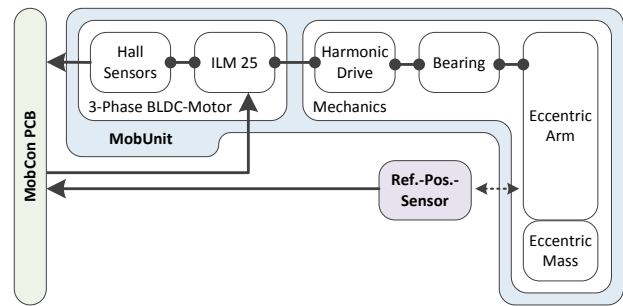


Figure 2. Block diagram of the mobility system.

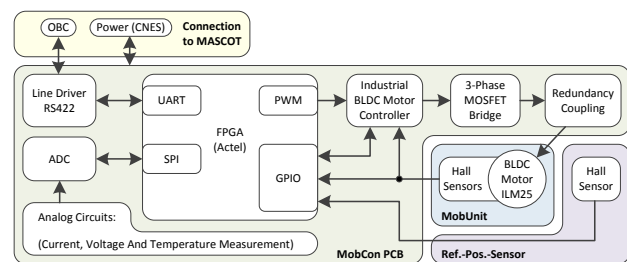


Figure 3. Block diagram of the electronics (MobCon).

The main control unit of the mobility is a flash based Microsemi (formerly Actel) FPGA. The main tasks are:

- communication by RS422 with OBC
- collecting measurement data of ADCs by SPI bus
- provide the control algorithm for the position control loop of the motor
- generate PWM signal for motor control
- calculate the eccentric arm absolute position by use of motor hall sensors and an additional reference position sensor
- realize safety monitoring of the unit

Since there is the harmonic drive gearing between motor and eccentric arm, the motor hall sensors do not show the absolute eccentric arm position. This is why there is an additional reference position sensor that detects reference magnetes mounted on the eccentric arm. After power on, an initialize sequence needs to be run so that the control algorithm can calculate the correct absolute position. In the following sections more details are shown on the hardware as well as on the electronics.

### 3. DETAILS ON THE HARDWARE

Fig. 4 shows a photo of the QM version of the mechanics. The design is the result of FEM analyses, simulation and the experience of the ROKVISS and DEXHAND Mission. Several parts of the MobUnit, were already tested and used in the DEXHAND. The suitable length of the eccentric arm and the weight of the eccentric mass were identified by mock-up tests and MBS simulations respectively. The mobility-mechanism is mounted on the MASCOT common electronics box because of mounting space, temperature and sealing requirements. The temperature range inside the E-box is from -20 up to approximately 40°C. The main part of the MobUnit is located inside the E-Box. The eccentric arm, the reference position sensor and a small part of the housing are situated in the actuation space of the arm, outside the E-Box.

Fig. 5 shows the CAD assembly of the MobUnit. The mechanism mainly consists of motor and gear (pink housing), bearing (orange housing), hall sensors, eccentric arm (purple), eccentric mass (brown) and the MLI stand-off (red). The hall sensor (grey) to detect the reference position of the eccentric arm is installed right in behind the arm.

The first model of the MobUnit was built up with standard components. This means that standard lubricated ball bearings were used as well as an off the shelf RoboDrive motor, and a standard steel Harmonic-Drive gear-box. The EQM of the MobUnit was built with a mix of standard and space proofed components. This means that Dicronite coated ball bearings were used as well as an off the shelf RoboDrive motor, and a Dicronite coated steel Harmonic-Drive gear-box. The material of the manufactured parts consists of aluminium 3.4364 (7075). All screws and other standard parts were made by stainless steel A2. The eccentric mass consists of a 99.97% tungsten alloy because of the very high density. The RoboDrive motor will be obtained in a special space version for the FM where the manufacturing process and testing is more strict and selected materials are used.



Figure 4. Photo of the qualification model of the motor and eccentric arm (mobility unit MobUnit).

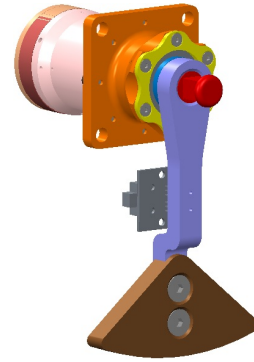


Figure 5. CAD image of the motor and eccentric arm (mobility unit MobUnit).

#### 3.1. Lubrication

A very important influence for the energy consumption and safe operation is the lubrication of the ball-bearings and the gearing. The lubrication in deep space mission has two tasks. The first is the minimization of the friction and the second one is the prevention of cold welding. Therefore a wrong chosen lubrication leads to a significant decrease of mission safety. Three different concepts were investigated.

##### Castrol Braycote

The first concept provides that all bearings and Harmonic-Drive parts were lubricated with Braycote. The lubrication, Castrol Braycote 602EF was chosen because of the good experiences made during the previous ROKVISS mission. Braycote 602EF is unique among the Braycote family of products because it contains a fine particle dispersion of MoS<sub>2</sub>. The disadvantage of Braycote is the considerable increase of the friction for high dynamics like in the proposed mechanism. In a test series this lubricant showed quite bad behaviour especially in cold environment. In summary it was decided to use better solutions if possible.

##### Cold-welding resistant materials combination

The second concept prevents cold-welding by well selected combinations of materials. The best solution is a combination of non-metallic and metallic materials. That leads to a cold-welding resistant solution. There is the possibility to take hybrid ball-bearings. These bearings consist of stainless-steel rings, Peek bearing cages and ceramic balls. Unfortunately it is not possible to select the material in this way for the harmonic-drive gear unit.

##### Cold-welding resistant coating

The third concept is to coat the surfaces of the mechanical parts with dry lubrication. For the MASCOT mission WS<sub>2</sub> (Dicronite) and MoS<sub>2</sub> were selected as the best solutions. WS<sub>2</sub> has a wide temperature range, extremely low outgassing behavior and a well-defined layer thickness. Dicronite was used in different space missions like the Mars-Exploration-Rovers. WS<sub>2</sub> forms no extensive coating but selective tungsten carbides. Therefore not enough cold welding prevention is given. MoS<sub>2</sub> has also

a wide temperature range, extremely low outgassing behavior and the lowest friction coefficient. MoS<sub>2</sub> was used in many space missions over the last 50 years. The extensive surface of MoS<sub>2</sub> guarantees prevention of cold welding. This is the main reason why MoS<sub>2</sub> was chosen as the best lubrication under the extreme conditions at the MASCOT mission.

### 3.2. Shaker test

The mechanical design of the hopping mechanism is simple, but a single mass oscillator. For this reason it is necessary to have a more detailed look at the performance and eigenfrequency of the MobUnit. To gain more experience with this behavior and in order to validate the FEM simulation, the MobUnit was tested on subsystem level. The test setup is shown in Fig. 6. After the first tests the y-direction turned out to be the most critical direction from which to stimulate the MobUnit. The MobUnit reached only 78 Hz eigenfrequency at the first subsystem shaker test at the shaker facility DLR Bremen (see Fig. 7). The mission requirements were an eigenfrequency above 100 Hz. The following two points show the reasons for the low eigenfrequency:

- Grooved ball bearings are much softer than expected.
- Connection between driving shaft and eccentric arm is too flexible.

Therefore a redesign of the MobUnit was necessary. The one modification is to change the grooved ball bearing against angular contact bearings with a wavespring. Thereby the prestressed bearings are very stiff and not susceptible regarding temperature changes. The other modification is a more inflexible design with one M5 screw to connect the shaft with the eccentric arm. With these two modifications the mobility was tested again. At the test bench the new setup showed an increase of the eigenfrequency up to 119 Hz (see Fig. 8).

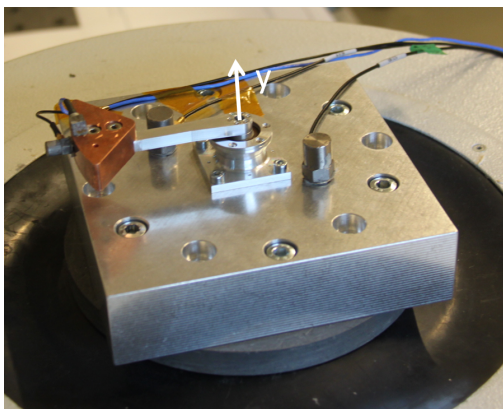


Figure 6. Test setup of the MobUnit mounted to the shaker.

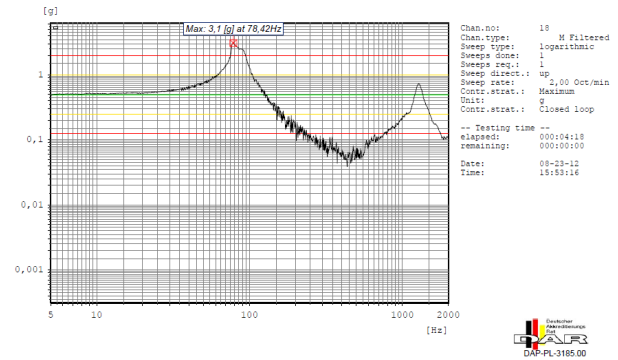


Figure 7. Shaker results with the first MobUnit prototype (eigenfrequency at 78 Hz).

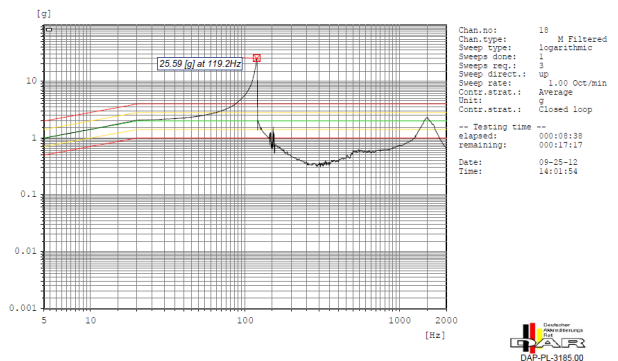


Figure 8. Shaker results with the redesigned MobUnit prototype (eigenfrequency at 119 Hz).

## 4. DETAILS ON THE ELECTRONICS

Not only size and weight limitations were the driver for developing an own electronics for the MASCOT project but also radiation and thermal issues. During the long cruise phase of MASCOT a very robust electronics hardware is mandatory. Whenever useful Components off the Shelf (COTS) were used to save space on the PCB. Furthermore ITAR free parts were used wherever possible.

### 4.1. Radiation Hard Components

#### Flash based FPGA

For the MASCOT electronics the flash based FPGA (RT3 series) from Actel was the best solution for our needs. Following topics made the decision towards the ITAR part Actel FPGA:

- small package (Ceramic Column Grid Array; CCGA)
- moderate power needs
- high system gate count
- no external peripheral units needed

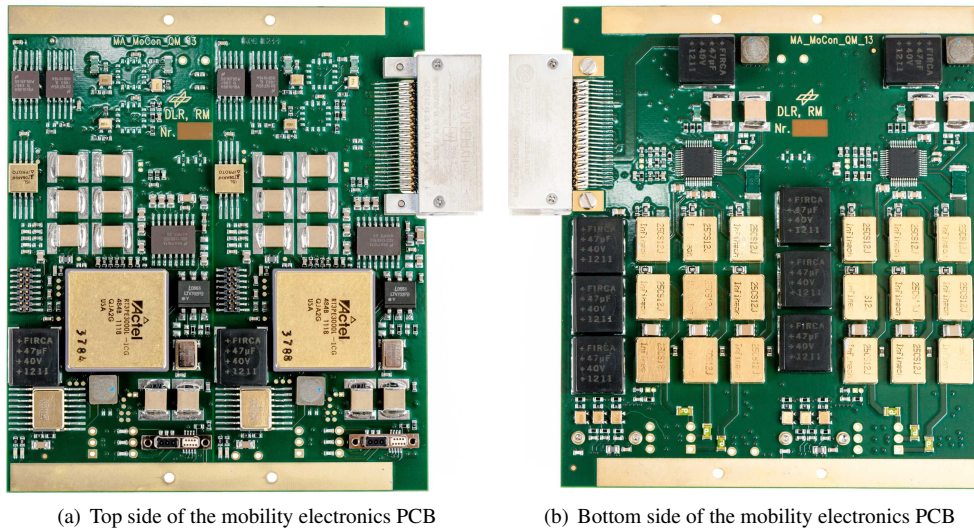


Figure 9. Photo of the qualification model PCB (top side and bottom side).

Other solutions for the control unit e.g. the usage of processors were not possible due to the limited available space. The following Fig. 9(a) shows the top side of the mobility electronics, with the FPGA on it.

#### MOSFETs

Infineon developed new radiation tolerant power MOSFETs (BUY25CSJ) based on DLR/ESA contracts (50PS0301, 50PS0409, 50PS0601, 50PS0903) within the European Component Initiative (ECI). These brand new power MOSFETs in the SMD0.5 package were selected due to their performance data and to overcome the ITAR restrictions. Furthermore the small package was helpful to realize a small and powerful motor drive unit. The following Fig. 9(b) shows the bottom side of the mobility electronics, where the MOSFETs of both redundancy levels are located.

#### 4.2. Components Off The Shelf

A central part of the MASCOT electronics is the motor drive electronics. For a Brushless DC (BLDC) motor 6 power MOSFETs must be driven and controlled in a proper way to optimize the performance of the motor and to minimize losses. The existing radiation hard components for BLDC motor control could not be used due to their huge form factor and the need for higher voltage levels than the MASCOT battery can supply. Therefore the Spin-In of a BLDC motor controller and MOSFET driver was treated as best way to meet the space and system requirements.

Military parts having a small form factor and high scale integration were not found, therefore a part for automotive application was used. For these parts an operating temperature range of  $-40^{\circ}\text{C}$  up to  $+150^{\circ}\text{C}$  is mandatory. This made it easy to meet the mission temperature requirements. Of course, radiation tests must be succeeded be-

fore this parts were treated as possible solution for a space mission.

#### TID results

For the MASCOT mission a total ionizing dose (TID) of 4.2 kRad (incl. margin) is expected for the electronics box. To provide additional margin for unforeseen events a minimum of 10 kRad was treated as criterion for the success / fail decision of the TID test. This test was performed at the Helmholtz Zentrum Berlin Wannsee, Germany [10]. The HZB offers a Cobalt 60 source with an activity of  $5.29 \cdot 10^{13} \text{ Bq}$  (June 2009). Multiple biased in-situ tests with a fully operable controller were performed at room temperature each. During these tests multiple parameters were measured.

At the end of the tests, all parts were fully operable at 14.5 kRad (water equivalent dose) which correlates to approx. 13 kRad(Si). Beyond this limit some parts stopped their operation due to the degradation of internal references which prevents the controller from erroneous operation.

The following Fig. 10 shows one result of the TID radiation tests. One measurement of the supply currents was done while the motor was rotating in clock wise direction (left graph). The next measurement shows the supply current while the motor was rotating counter clock wise (right graph). Although the supply current after the irradiation doubles almost the value of the unirradiated parts, we saw no functional errors or discovered any thermal problems. Please note that the dose is noted as water equivalent dose value.

#### Proton test results

Similar to the TID test, the proton tests were performed at the HZB, too. The HZB offers protons up to 68 MeV [11]. For this test campaign a fluence of

$$\Phi_{Test} = 1.7 \cdot 10^{10} \frac{\text{Protons}}{\text{cm}^2}$$

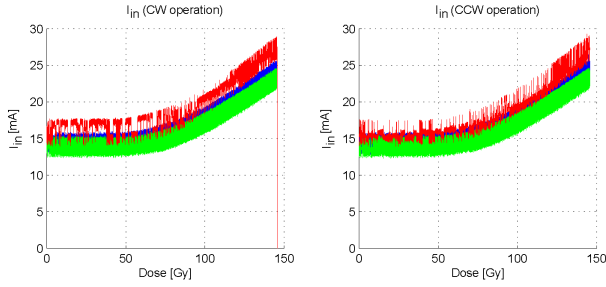


Figure 10. Motor controller TID test summary.

within five different proton energies equally spaced from 30 MeV up to 68 MeV were applied to the controller. During the biased in-situ tests several parameter were measured, but despite of the tachometer signal no significant disturbances or Single Event Functional Interrupt (SEFI) were monitored. Within the MASCOT project the speed information is derived from the hall sensors which are used for motor commutation by the control unit. Therefore this effect won't affect the performance of the MASCOT electronics.

The following Fig. 11 shows the hall sensor supply voltage which is provided by the motor controller in more detail. For this plot, all proton subtest measurements were concatenated starting with the 68 MeV test results down to 30 MeV results. Therefore the x-axis is scaled in "Samples" which could be transferred to seconds of test time by factor of two. In general, some minor spikes could be detected, but the major degradation is based on the deposited total dose which was injected during the irradiation with protons.

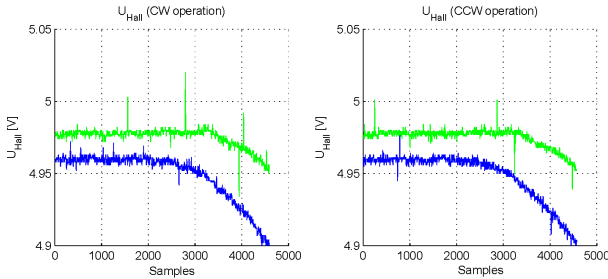


Figure 11. Motor controller proton test summary.

### Ion test results

After delidding of the parts the ion tests were performed at the radiation effects facility in Jyväskylä, Finland [12]. Up to an effective LET(Si) of  $27.4 \frac{\text{MeV}}{\text{mg cm}^2}$  (at the bragg peak) no disturbances, SEFIs or Single Event Latchups (SEL) were monitored. Only a few voltage spikes on analogue input or output voltages could be monitored. As an example for the seen effects the hall sensor supply voltage is shown in the next Fig. 12. The left graph shows the result of sample 1 while the right graph shows the result of sample 2.

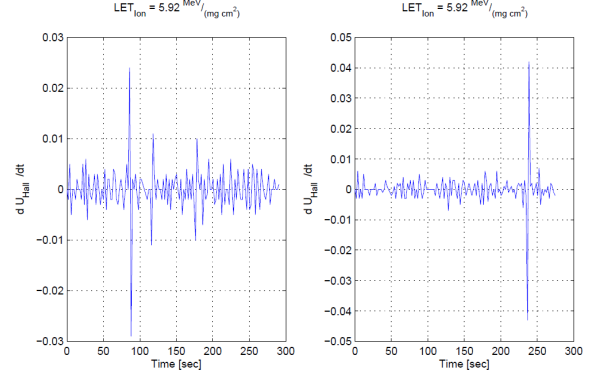


Figure 12. Motor controller ion test summary.

## 5. DETAILS ON THE CONTROL ALGORITHM

The controller must ensure the movement of the eccentric arm within given constraints to generate a defined jerk for the MASCOT system. Therefore no overshoot for the position must occur. The trajectory can be separated into the three phases acceleration, constant speed and deceleration (see Fig. 13). The time periods are dependent on the parameters acceleration, deceleration, maximum velocity, start and end position. Assumed that starting position and

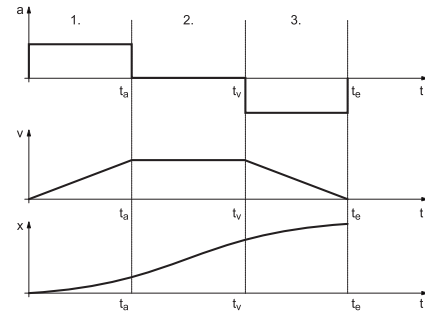


Figure 13. Movement phases of the eccentric arm.

velocity are zero at  $t = 0$ , meaning that the system is at standstill in the beginning, Eqs. (2) show the basic calculation of the trajectory.

$$\begin{aligned} v &= \int_0^t a_{max} \cdot d\tau = a_{max} \cdot t \\ x &= \int_0^t v \cdot d\tau = \frac{1}{2} \cdot a_{max} \cdot t^2 \end{aligned} \quad (2)$$

Both equations can be solved for the time to get the desired velocity (3). This way the parameters acceleration, deceleration, speed limit for the constant speed phase, starting position, end position are sufficient to characterise the complete trajectory of the eccentric arm and to ensure precise movement.

$$\begin{aligned} \Delta x &= x_{des} - x_{act} \\ v_{des} &= \sqrt{2 \cdot a_{max} \cdot |\Delta x|} \cdot \text{sign}(\Delta x) \end{aligned} \quad (3)$$

The difference of desired and actual position leads directly to the desired velocity. This value is computed

online by the position controller. Because of massive non-linear friction an additional velocity PI-controller is used to prevent steady state position difference. Fig. 14 shows a block diagram of the cascaded controllers. The param-

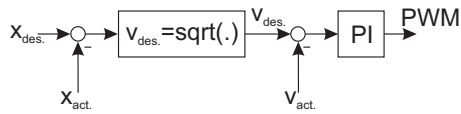


Figure 14. Position controller and PI velocity controller cascaded to compute the necessary motor actuating signals.

eters for the trajectory are taken from simulation results. Due to the very low gravity on the asteroid it is very difficult to extract that data from a test bench in the laboratory. Only scaled measurements were taken in the laboratory to validate the simulation results.

## 6. CONCLUSION

The presented hardware is developed and tested for the rough environments in space applications. Furthermore it shows very high power density and two complete redundant signal paths. The use of brushless motors leads to a much higher torque output at the given weight limitation. With the better efficiency of the drive train, compared to brushed motors, less power consumption is required. This is of great advantage when the system is powered by battery only.

The module may also be used for different other applications like for example a pan-tilt drive [6] or even a small traction system. With slight modification the system is also scalable to an increased power output. The main limitation is of course given by the environmental conditions as it is necessary to dissipate the heat loss. For low gravity missions in future it would also be possible to extend the hopping concept by additional eccentric arms arranged orthogonally. This way a more accurate hopping performance could be achieved which leads to more precise science possible on asteroids. With more degrees of freedom the system gets more robust and the dependency on the mass distribution of the system is decreased.

## REFERENCES

[1] G. Hirzinger, K. Landzettel, D. Reintsema, C. Preusche, A. Albu-Schaeffer, B. Rebele, and M. Turk. ROKVISS robotics component verification on ISS. In *8th Int. Symposium on Artificial Intelligence, Robotics and Automation in Space - iSAIRAS*, Munich, Germany, 2005.

[2] A. Albu-Schaeffer, W. Bertleff, B. Rebele, B. Schaeffer, K. Landzettel, and G. Hirzinger. ROKVISS robotics component verification on ISS current experimental results on parameter identification. In

*International Conference on Robotics and Automation - ICRA*, pages 3879–3885, Orlando, USA, 2006.

[3] B. Schaefer, K. Landzettel, and G. and Hirzinger. ROKVISS: orbital testbed for tele-presence experiments, novel robotic components and dynamics models verification. In *8th Symposium on Advanced Space Technologies in Robotics and Automation (ASTRA)*, ESA/ESTEC, Noordwijk, Netherlands, Nov. 2004.

[4] A. Wedler, M. Chalon, K. Landzettel, M. Goerner, E. Kraemer, G. Gruber, A. Beyer, H.-J. Sedlmayr, B. Willberg, W. Bertleff, J. Reill, M. Grebenstein, M. Schedl, A. Albu-Schaeffer, and G. Hirzinger. DLR's dynamic actuator modules for robotic space applications. In *41th Aerospace Mechanisms Symposium AMS*, Pasadena, USA, May 2012.

[5] A. Wedler, M. Chalon, A. Baumann, W. Bertleff, A. Beyer, R. Burger, J. Butterfass, M. Grebenstein, R. Gruber, F. Hacker, E. Kraemer, K. Landzettel, M. Maier, H.-J. Sedlmayr, N. Seitz, F. Wappler, B. Willberg, T. Wimboeck, F. Didot, and G. Hirzinger. DLR's space qualifiable multi-fingered DEXHAND. In *11th Symposium on Advanced Space Technologies in Robotics and Automation (ASTRA)*, volume 11, page Session 3a, ESA/ESTEC, Noordwijk, Netherlands, 12 - 14 April 2011.

[6] A. Wedler, A. Maier, J. Reill, C. Brand, H. Hirschmueller, M. Suppa, A. Beyer, and R. Haarmann. Pan/Tilt-Unit as a perception module for extra-terrestrial vehicle and landing systems. In *12th Symposium on Advanced Space Technologies in Robotics and Automation (ASTRA)*, ESA/ESTEC, Noordwijk, Netherlands, May 2013.

[7] C. Dietze, F. Herrmann, S. Kuß, C. Lange, M. Scharinghausen, L. Witte, T. van Zoest, and H. Yano. Landing and mobility concept for the small asteroid lander MASCOT on asteroid 1999 ju3. In *61st International Astronautical Congress IAC*, Prague, Czech Republic, 2010.

[8] F. Herrmann, S. Kuß, and B. Schaefer. Mobility challenges and possible solutions for low-gravity planetary body exploration. In *11th Symposium on Advanced Space Technologies in Robotics and Automation*, ESA/ESTEC, Noordwijk, Netherlands, 12 - 14 April 2011.

[9] RoboDrive. Website of the RoboDrive GmbH company. online available: <http://www.robodrive.de/>.

[10] Helmholtz Zentrum Berlin Wannsee. Cobalt-60 source. [http://www.helmholtz-berlin.de/angebote/industrie/kobalt/index\\_en.html](http://www.helmholtz-berlin.de/angebote/industrie/kobalt/index_en.html), 2013.

[11] Denker A., Rethfeldt C., Roehrich J., Cordini D., Heufelder J., Stark R., and Weber A. Status of the HZB cyclotron. In *Proc. of the Cyclotrons 2010 Conference*, pages 78–80, 2011.

[12] University of Jyvaskyla. Radiation effects facility - RADEF. <https://www.jyu.fi/fysiikka/en/research/accelerator/radeef>, 2013.